GPS Receiver Architecture Effects on Controlled Reception Pattern Antennas for JPALS

David S. De Lorenzo, *Stanford University*
Jennifer Gautier, *Stanford University*
Per Enge, *Stanford University*
Dennis Akos, *University of Colorado at Boulder*

BIOGRAPHY

David De Lorenzo is a member of the Stanford University GPS Laboratory, where he is pursuing a Ph.D. degree in Aeronautics and Astronautics. He received a Master of Science degree in Mechanical Engineering from the University of California, Davis, in 1996. David has worked previously for Lockheed Martin and for the Intel Corporation.

Dr. Jennifer Gautier is a Research Associate in the GPS Laboratory at Stanford University, where she leads the Lab's research program for the Joint Precision and Approach Landing System (JPALS). She received the Bachelor's degree in Aerospace Engineering from Georgia Tech and completed the Master's and Ph.D. degrees in Aeronautics and Astronautics at Stanford University. Dr. Gautier has worked for Lockheed, Honeywell Labs, and Trimble Navigation, Ltd.

Dr. Per Enge is a Professor of Aeronautics and Astronautics at Stanford University, where he is the Kleiner-Perkins, Mayfield, Sequoia Capital Professor in the School of Engineering. He directs the GPS Research Laboratory, which develops satellite navigation systems based on the Global Positioning System. Dr. Enge has received the Kepler, Thurlow, and Burka Awards from the Institute of Navigation for his work. He is a Fellow of the Institute of Navigation and the Institute of Electrical and Electronics Engineers.

Dr. Dennis M. Akos is an Assistant Professor with the Aerospace Engineering Science Department at the University of Colorado at Boulder. He also has served as a faculty member with the Luleå Technical University, Sweden, and as a Research Associate in the GPS Laboratory at Stanford University. Dr. Akos completed the Ph.D. degree in Electrical Engineering at Ohio University within the Avionics Engineering Center.

ABSTRACT

Stanford University is developing a controlled reception pattern antenna (CRPA) array with beam-steering/adaptive-null-forming capabilities as part of a research testbed to evaluate CRPA algorithms and software tools, and their effects on GPS signals and satellite tracking performance. The correlation power peak ratio (CPPR), defined as the ratio of the largest correlation peak to the next-highest peak (more than 1-chip away), is used to evaluate tradeoffs between characteristics of multi-element GPS antenna systems. Based on this signal-quality-based metric, a trade-space was identified and simulations were developed to evaluate trades in front-end architecture for the steered-beam testbed. Specifically, the order of beam-forming and correlation operations was found to not introduce appreciable differences in the CPPR. However, the number of analog-to-digital (A/D) quantization levels and the A/D converter (ADC) dynamic range vs. signal amplitude (e.g., the signal variance for white-noise-dominated signals) would cause changes in the CPPR – signals were degraded for fewer numbers of A/D quantization bits (most notably for a 1-bit ADC) and for sub-optimal ADC dynamic range. The conclusion was that the CRPA front-end hardware and A/D conversion plan are feasible with integrated components and post-correlation beam-forming, even given the limitations in sampling frequency and numbers of A/D quantization levels in off-the-shelf components. Finally, a further program of numerical simulations is proposed which will lead to additional system design improvements and development of a software-defined radio.

INTRODUCTION

Stanford University is leading a multi-disciplinary, multi-university team in support of Joint Precision and Approach Landing System (JPALS) system definition and trade studies. JPALS is a United States Navy and Air Force project to provide local-area augmentation of the

on-board GPS navigation solution for pilots on approach to aircraft carrier, fixed base, and tactical airfields.

A number of advanced technologies are being evaluated in order to meet strict accuracy, integrity, continuity, and availability goals for JPALS, given the presence of a hostile jamming and harsh multipath environment. One of the technologies being studied is a controlled reception pattern antenna (CRPA) array with beam-steering/adaptive-null-forming capabilities. Of particular importance in CRPA design and evaluation are the impacts to beam/null pointing accuracy, signal acquisition, and carrier phase resolution from analog-to-digital (A/D) quantization and PRN-code correlation architecture.

In order to study CRPA algorithms and their effects on GPS signals and satellite tracking performance, a multi-antenna signal acquisition simulator was developed that allows control of array geometry, sampling methodology (mixing and down-conversion, sampling frequency, and A/D quantization), S/V line-of-sight vector, antenna main-beam vector, injected noise, and correlation architecture. This paper describes specifically the simulations done to date – simulations to quantify the impact from A/D quantization, beamforming vs. correlation architecture, and A/D converter (ADC) dynamic range vs. noise variance mismatch. Other actual system imperfections, while recognized, are not explicitly addressed in this study. In addition, noise was injected as additive white Gaussian noise (AWGN); CW jammers will be considered later. Finally, a single main-beam was formed by appropriate signal weighting and phase-shifting – null-forming/null-steering will be treated subsequently.

The final goal of the current analysis is to drive selection of front-end hardware for a multi-element antenna array (Figure 1). Front-end architectures may be broadly classified based on the level of component integration [Akos & Tsui, 1996], with the requirement that the front-end design makes possible scale-up from a single-antenna system to multi-element arrays. Front-end components such as filters, amplifiers, and mixers may be selected individually [Gromov, 2002] – this approach allows the maximum flexibility over filter characteristics, downconversion frequencies, and A/D specifications, although at a penalty to cost and ease of integration/calibration. Conversely, a solution may be chosen that uses identical copies of off-the-shelf application-specific integrated circuits (ASICs) [Prades, 2004] – advantages of this approach include low cost and ease of assembly, although with disadvantages to flexibility, number of A/D quantization levels, and potentially using very narrow filter bandwidths.

CRPA BACKGROUND

Multi-element antenna system technology is well-described in the literature, particularly as applied to beamforming, null-steering, and gain-pattern computation [Applebaum, 1976; Stutzman & Thiele, 1998; Kim & Iltis 2002]. Similarly, signal acquisition, tracking, and the ability to achieve a navigation solution are well-documented; this includes weak-signal acquisition, interference mitigation and suppression, and multipath rejection [Amoroso, 1983; Amoroso & Bricker, 1986; Spilker, 1996; Spilker & Natali, 1996; Van Dierendonck, 1996; Ward, 1996a; Ward, 1996b; Akos, 2000; Misra & Enge, 2001]. One challenge of the present work was to characterize the impact to GPS signal quality from the CRPA array processing and beamforming algorithm – not just to address gain or attenuation of the signal, but also to capture the impact of these effects on the C/A code pseudo-random noise (PRN) autocorrelation process and carrier phase discrimination. Ultimately, the final measure of the performance of any GPS processing system is its ability to deliver information to a navigation algorithm.

So, for an *n*-element receiving array, a beam is formed either by applying appropriate time delays to the signal

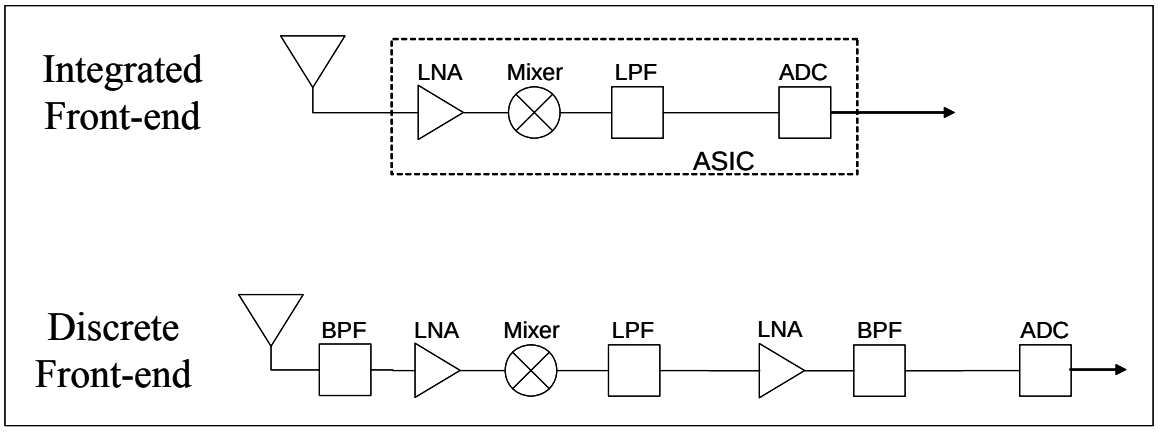

Figure 1. GPS front-end architectures.

transmission paths prior to summation or by multiplying the signal vector by a complex weighting (i.e., phase-shifting) vector and then taking a summation. This time-shifting or phase-shifting can occur either as pre-correlation beamforming, where the shifts are applied to the separate satellite signals directly, or as post-correlation beamforming, where the beamforming operation occurs after the complex correlators operate on the antenna signals [Granados, 2000] (Figure 2). Additionally, note that for pre-correlation beamforming the operation occurs at the sampling frequency (~MHz speeds) while for post-correlation beamforming the operation occurs at the integrate-and-dump frequency (~kHz). (There are other implications in terms of weak signal acquisition, but discussion of these is deferred to the Conclusion.)

The time delay for the i^{th} element with respect to the array center is found as the dot-product of that element's baseline vector with the boresight unit-vector, and divided by the wave propagation speed:

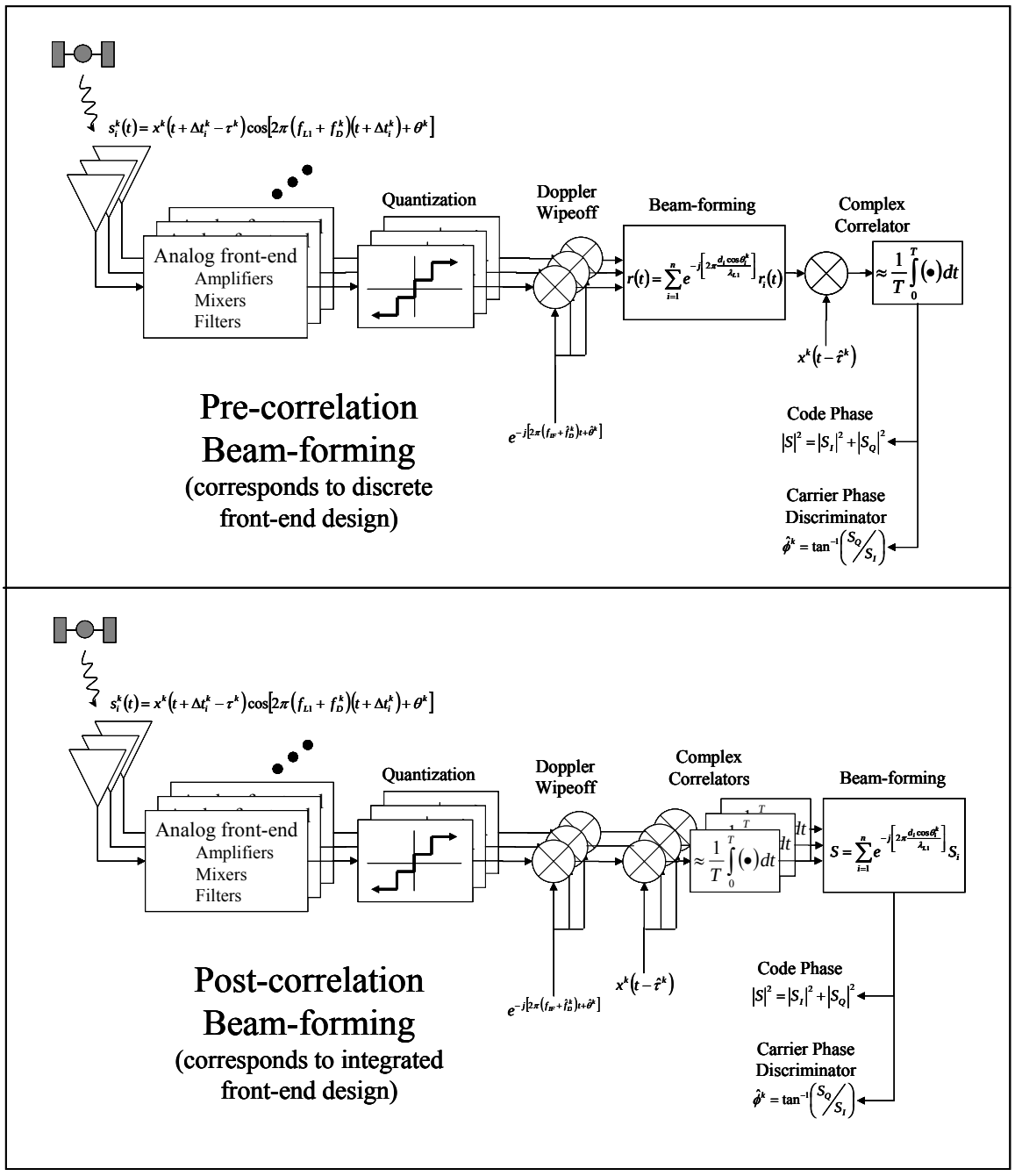

Figure 2. GPS beamforming and correlation architectures.

$$dt_i = \frac{\vec{p}_i \cdot \hat{r}_{boresight}}{c} \qquad \text{[Eq. 1]}$$

The complex weights are likewise found using a dot-product operation:

$$w_i = \exp\left[-j\left(2\pi \frac{\vec{p}_i \cdot \hat{r}_{boresight}}{\lambda_{L1}} \right) \right] \qquad \text{[Eq. 2]}$$

Finally, the array factor magnitude for isotropic, isolated, equal-current elements may be calculated as a function of signal-arrival azimuth and elevation [Stutzman & Thiele, 1998]:

$$AF(\theta,\phi) = \left| \sum_{i=1}^{n} \exp\left[j \frac{2\pi}{\lambda_{L1}} \left(\vec{p}_i \cdot \hat{r}_{\theta,\phi} - \vec{p}_i \cdot \hat{r}_{boresight} \right) \right] \right| \qquad \text{[Eq. 3]}$$

The array gain pattern can be determined according to [Eq. 3], with examples for a 7-element planar array with λ/2 inter-element separation and for a variety of boresight directions shown in Figure 3. For a boresight azimuth of 45°, the figure shows gain patterns for elevation values of 20°, 45°, and 80°. In the 3-D depiction of the first row, the shape corresponds to the array gain and the color scale is in dB. The second row of figures shows a 2-D slice, or section, through the 3-D gain plot, in this case through the boresight azimuth of 45°. Finally, the last row of figures shows the dB-gain color scale of the upper hemisphere (+z-axis) projected onto a 2-D polar plot. In this way, the entire information of the 3-D plot is preserved in a 2-D representation, clearly showing the characteristics of the array main-beam, sidelobes, and nulls.

EVALUATION METRIC

Given the ability to create a CRPA beam in a desired direction, the next issue is the array gain impact on the incoming GPS signals. For a GPS signal entering the array, for example along the boresight or from an array null, the correlation between the incoming signal and the receiver-generated replica C/A code can be computed as a function of code-phase offset (Figure 4). For a mid-elevation beam (45° elevation), pre-correlation beamforming, and floating-point signals (e.g., ideal A/D quantization), a strong correlation peak is apparent for 1ms non-coherent correlation and C/N0 of 45 dB-Hz, as well as for 3ms integration and C/N0 of 35 dB-Hz. Likewise, for signals entering from an array null (in this case gain less than -16 dB), there is suppression and acquisition fails (e.g., no well-defined correlation peak at the correct code-phase offset).

Now, it is desirable to define a signal-quality-based metric with which to quantify changes to different aspects of the CRPA system. A logical metric is one that includes explicit accounting for the correlation properties of the GPS PRN spreading codes – for this reason, an

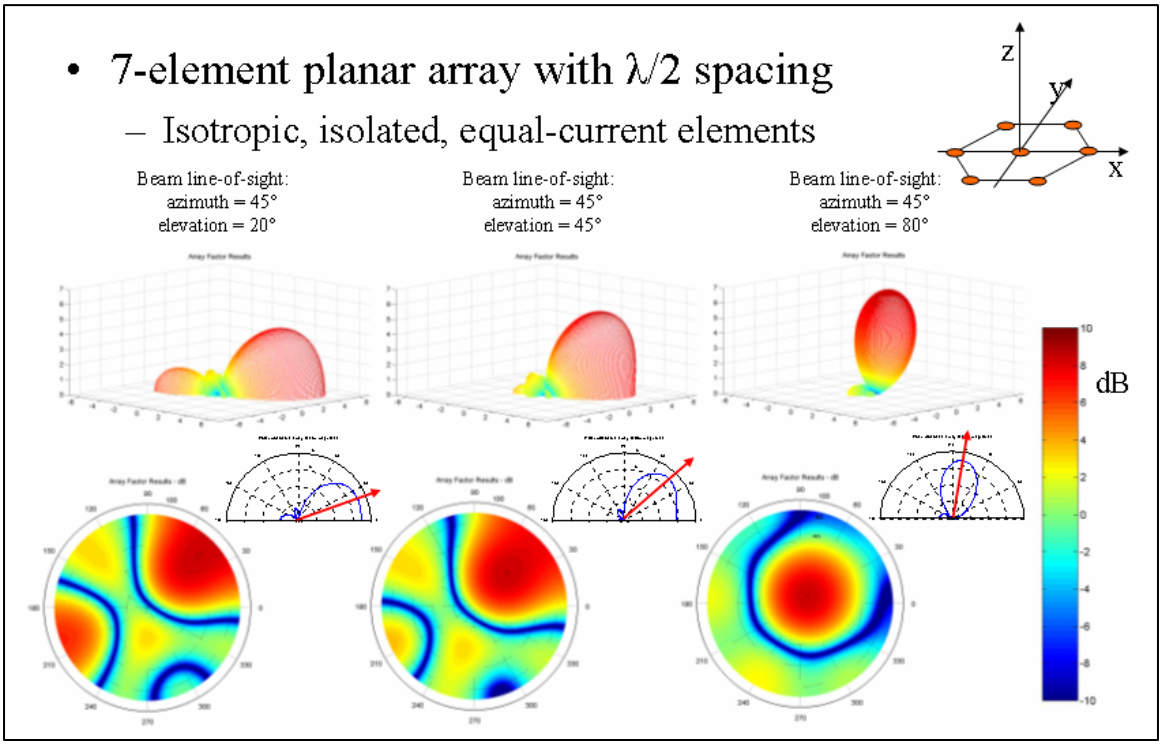

Figure 3. Array gain patterns for 7-element CRPA.

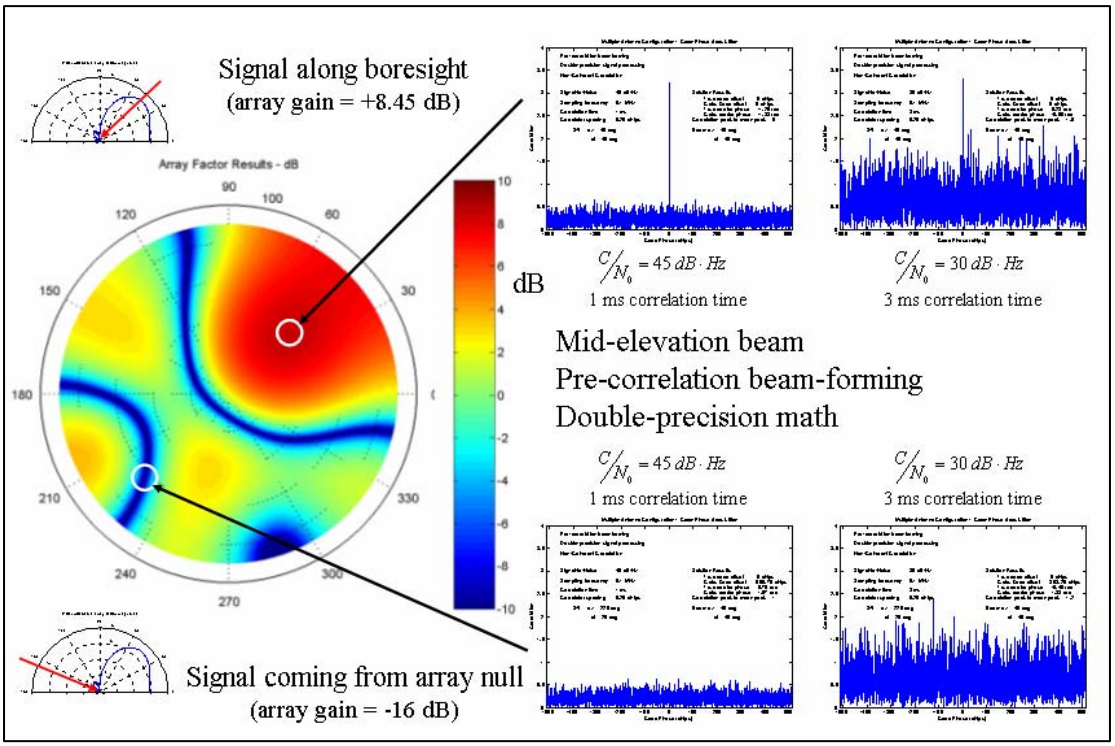

Figure 4. GPS signal acquisition: correlation vs. arrival direction, 7-element CRPA.

"acquisition-based" metric is used [Jung, 2004], following from the development of the previous paragraph. For a given system scenario and acquisition processing, the ratio of the largest correlation peak to the next-highest peak (more than 1-chip away) is computed; this allows display of signal reception vs. boresight for a variety of system parameters. Successful detection of the PRN code is achieved when this correlation power peak ratio (CPPR) exceeds 1.4-1.6. Adoption of this standardized measure allows acquisition-related parameters (e.g., integration time, sampling frequency, interference suppression, etc.) to be decoupled from the array-specific analysis – the impact to the CPPR from changing these acquisition parameters can be treated separately from CRPA algorithm/processing changes. Therefore, simulations will consider a satellite acquisition scenario using a nominal 7-element antenna array with λ/2 inter-element separation, direct digitization to 6.1 MHz, 1ms non-coherent correlation, and varying levels of AWGN input.

Accordingly, the CPPR may be computed for all incident azimuth and elevation values, as shown in the lower left plot in Figure 5. However, a more useful curve may be created by sectioning the gain and CPPR plots, i.e., by taking a slice through the boresight azimuth – this will allow direct comparison between signal reception/suppression performance and system/noise characteristics across trials. For example, CPPR vs. signal arrival direction for a 45° elevation boresight can be shown for elevation values from 0° (the near horizon), through 90° elevation (zenith, or directly overhead), and over to the far horizon at 180°. The characteristics of the CPPR plot in the lower right of Figure 5 are similar to the gain pattern in the upper right, showing that signal reinforcement/suppression properties of the array reveal themselves through the CPPR.

SIMULATIONS AND RESULTS

Given the previous development, it is now possible to compare the effects of various front-end architecture choices. First, the impact due to signal quantization (e.g., the number of bits of A/D resolution) on the ability to acquire a GPS signal and to determine accurately its carrier phase may be evaluated. Signals are treated at either the full numerical precision of the simulation platform, or pass through a 1-bit, 2-bit, or 3-bit quantization stage.

The GPS signals are buried in noise; whether looking at a time-series or at an amplitude probability density function, the signal appear noise-dominated – it is only the C/A code correlation process that allows the underlying structure to appear. The sampling and quantization process results in a loss of information due to the conversion from signals continuous in both time and amplitude to discrete samples. However, sampling frequency, record length, and integration time effects will

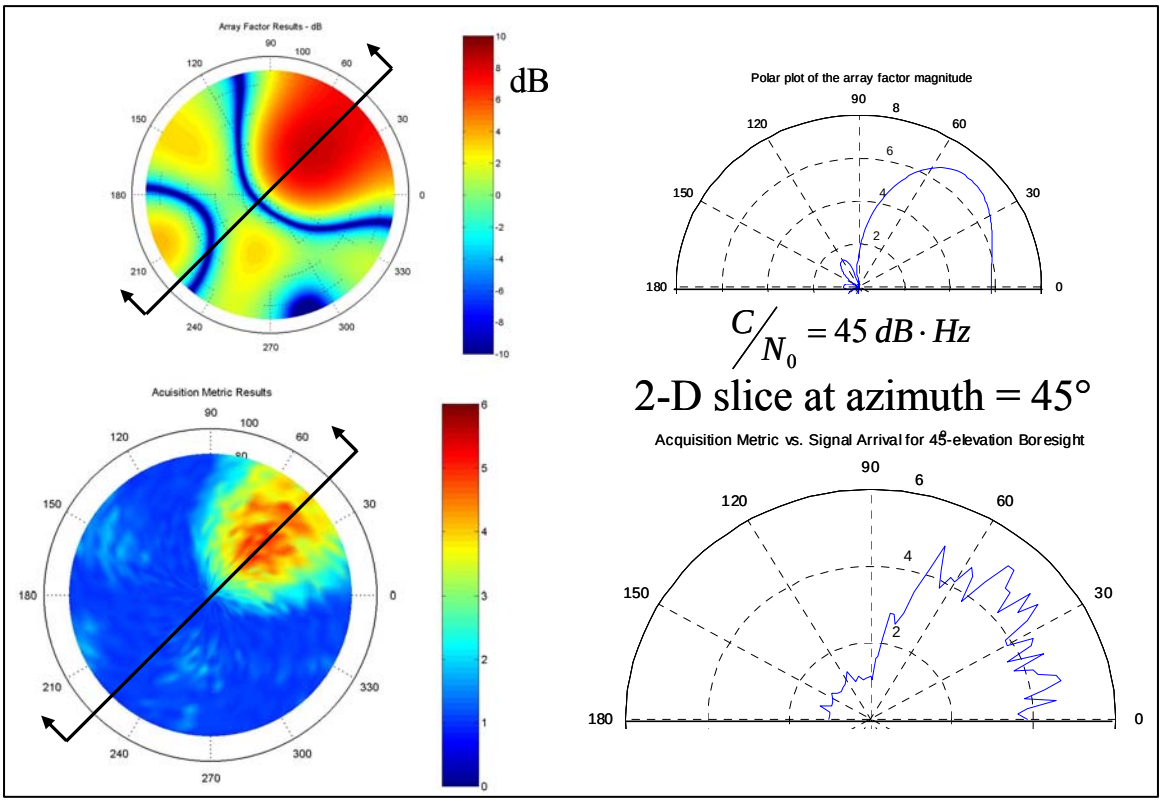

Figure 5. GPS signal correlation metric vs. arrival direction, 7-element CRPA. Left-side shows entire sky (gain and correlation); right-side shows a section at boresight azimuth.

not be addressed here; these areas are well-treated in the literature.

An ideal ADC would preserve of all the amplitude information content of the input sampled waveform – there would be a 1:1 mapping from analog input to digital output (Figure 6). In contrast, a 1-bit ADC stores only the sign of the input signal; a 2-bit midriser ADC stores 2 positive and 2 negative values of the input sampled waveform; and so-on for greater numbers of quantization

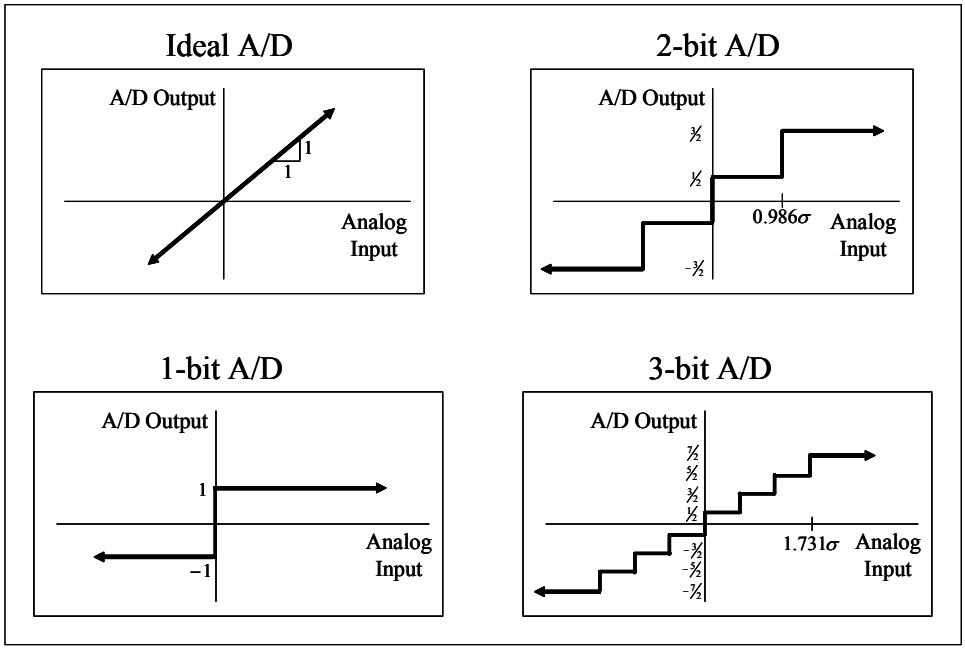

Figure 6. Analog-to-digital converter input vs. output.

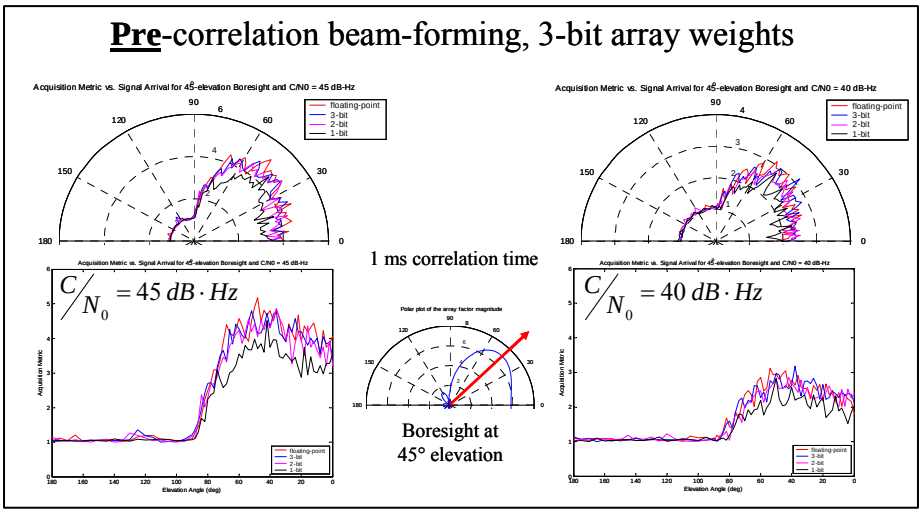

Figure 7. Effect of A/D converter bit resolution – Pre-correlation beamforming.

levels. In general, for an *n*-bit ADC, 2^n levels may be distinguished.

There is degradation to the signal associated with quantization, not only from the loss of information due to discretization but also a potential further loss due to a mismatch between the dynamic range of the ADC and the signal characteristics coming out of the analog front-end (other losses, associated with non-ideal ADC characteristics, are excluded from analysis here). For example, the optimum threshold for the upper quantization transition of a 2-bit converter is approximately 0.986σ, where σ is the standard deviation of the input signal to the ADC; the final quantization threshold for a 3-bit converter is approximately 1.73σ [Bastide, 2003].

To look at signal degradation as a function of the number of quantization bits in the ADC, simulations were run for various signal arrival directions in elevation along the array boresight azimuth. Then the CPPR was compared for a floating-point (ideal) converter, and 3-bit, 2-bit, and 1-bit converters. For pre-correlation beamforming, and assuming 3-bits for the array weights, there is a reduction in the CPPR with fewer A/D quantization levels (Figure 7). However, while there is degradation for fewer quantization levels, there is not an appreciable widening of the main beam, although this is likely a consequence of applying the same 3-bit array weighting to all incoming signals (irrespective of the number of bits in the ADC).

Likewise, for post-correlation beam-forming, in this case carrying floating-point (ideal) array weights because of the lower (~KHz) post-correlation data throughput, there is a reduction of the CPPR with fewer quantization levels (Figure 8).

Finally, comparing pre-correlation and post-correlation

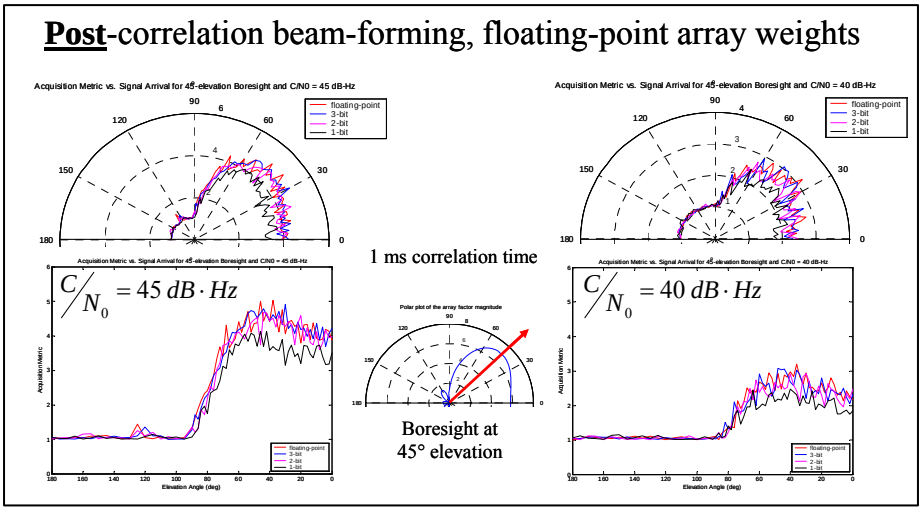

Figure 8. Effect of A/D converter bit resolution – Post-correlation beamforming.

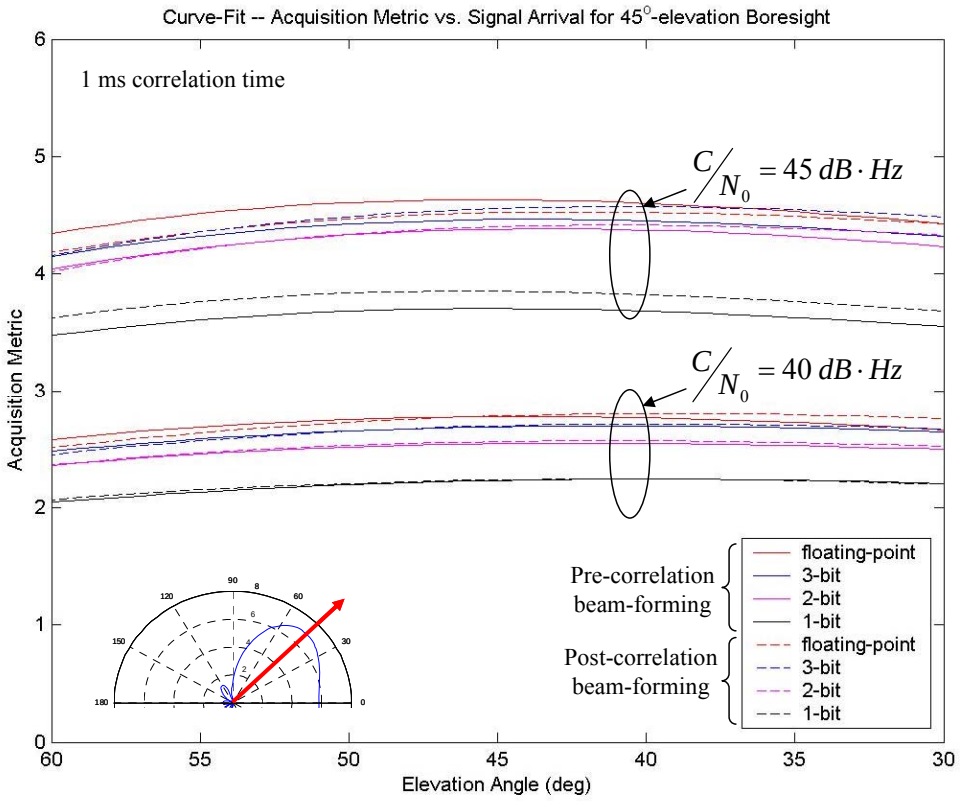

Figure 9. Correlation metric vs. A/D resolution and correlation architecture.

beamforming for various numbers of A/D quantization levels, there is no appreciable difference between architectures (Figure 9). In fact, the smoothed results of CPPR in the vicinity of the antenna boresight show minimal degradation for 3-bit and 2-bit converters, with the CPPR falling off appreciably only for a 1-bit converter. However, this result holds only for AWGN, not for a CW jammer.

Regarding the effects of mismatched dynamic range, comparisons can be made between the optimal values of quantization threshold given above, and sub-optimal values. For example, for a 2-bit ADC where the optimal value of the quantization threshold is 0.986σ, the effects to CPPR for sub-optimal values can be investigated. A further degradation in signal-to-noise ratio of ~1dB can be expected when changing the threshold from 0.986σ (the optimal value) to either 0.2σ on the low-end or 2.3σ on the high-end [Bastide, 2003], with the performance approaching that of the 1-bit ADC in the limit.

For pre-correlation beamforming, there is a reduction in the CPPR with mismatched ADC dynamic range (Figure 10). Likewise, for post-correlation beam-forming, there is a reduction of the CPPR with mismatched ADC dynamic range (Figure 11). Finally, comparing pre-correlation and post-correlation beamforming with mismatched dynamic range, there is no appreciable difference between architectures (Figure 12). However, the degradation is greater at lower values of C/N0 and would be more pronounced still for a CW jammer.

CONCLUSIONS AND FUTURE WORK

Based on the simulations described herein, it is found that the CPPR is sensitive to A/D quantization, decreasing with fewer numbers of A/D quantization levels as well as with mismatched ADC dynamic range. It was found that pre-correlation vs. post-correlation beamforming architecture does not introduce appreciable differences in CPPR, and this conclusion was tested across various numbers of A/D quantization levels, although assuming high-resolution beamforming (at least 3-bit beamforming weights).

The results of this study are critical to the design of actual front-end hardware and to establish a sampling plan for the CRPA testbed under development. According to the findings described herein, it appears that the CRPA front-end hardware and A/D conversion plan are feasible with integrated components and post-correlation beam-forming, even given the limitations in sampling frequency and numbers of A/D quantization levels in off-the-shelf components. Immediate next steps include hardware architecture design and construction as well as further simulations testing beam-steering/adaptive-null-forming

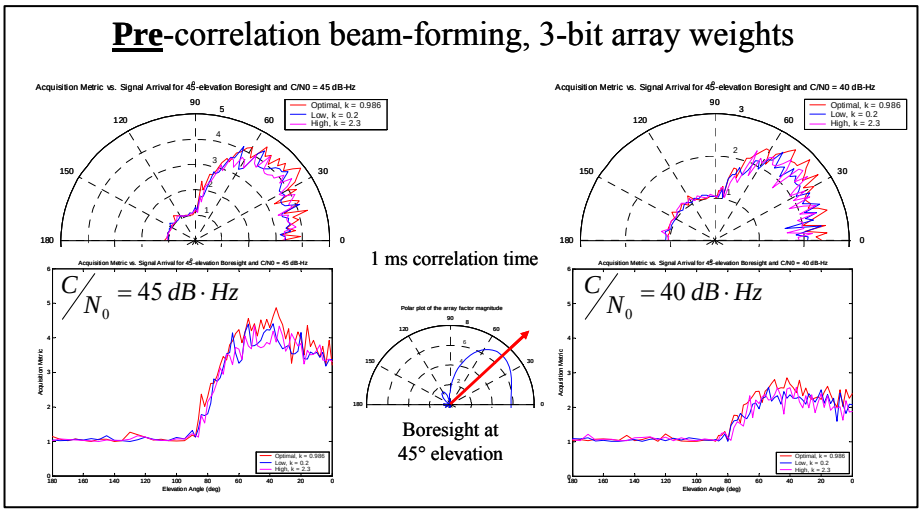

Figure 10. Effect of ADC dynamic range mismatch – Pre-correlation beamforming.

performance as influenced by quantization and correlation choices. Other important factors to be addressed include initial array calibration (and possibly a real-time monitor) and assessment of channel biases on array performance [Kim, 2004].

The findings of this study are limited to the case for AWGN input, no other system imperfections, and no null-forming/null-steering. Introducing these further parameters into the simulation environment will comprise a parallel stage of research to hardware design and construction. In addition, the impact from reduced fidelity of the beamforming weights, the benefit from more elements in the antenna array and possibly other choices of array geometry, and the impact of front-end hardware elements (e.g., filters and amplifiers) will be studied.

One other comment will be offered, given the attractive behavior of post-correlation beamforming and its suitability for software-defined radios. Post-correlation beamforming allows many possible signal arrival directions to be tested during the acquisition phase by operating numerous times on the same correlator outputs – basically conducting a search over signal arrival direction by appropriate choice of weighting vectors. This could be a useful option in cold-start or unknown-attitude/ephemeris scenarios with low C/N0. Alternatively, C/A code replicas from several PRN sequences may be combined as input to the correlators – this option allows rapid searching of the code-space across several satellites and signal arrival directions in cold-start scenarios with moderate-to-high C/N0.

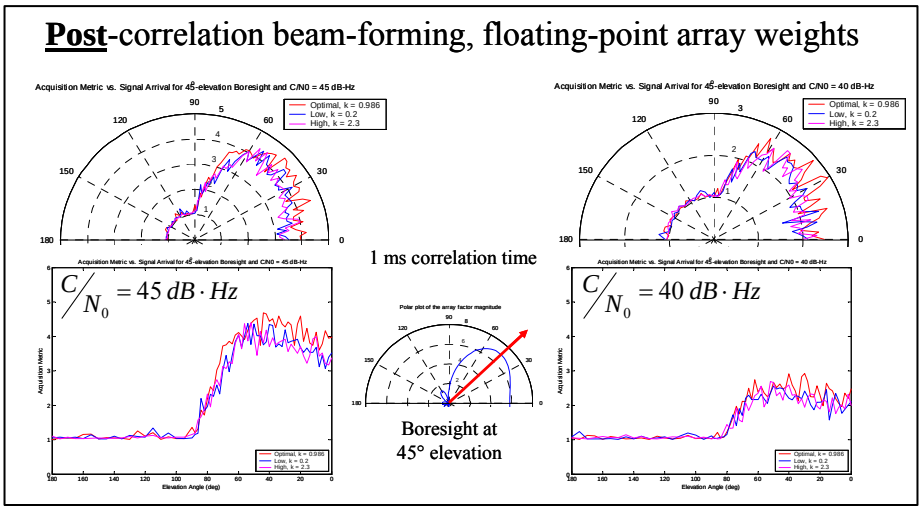

Figure 11. Effect of ADC dynamic range mismatch – Post-correlation beamforming.

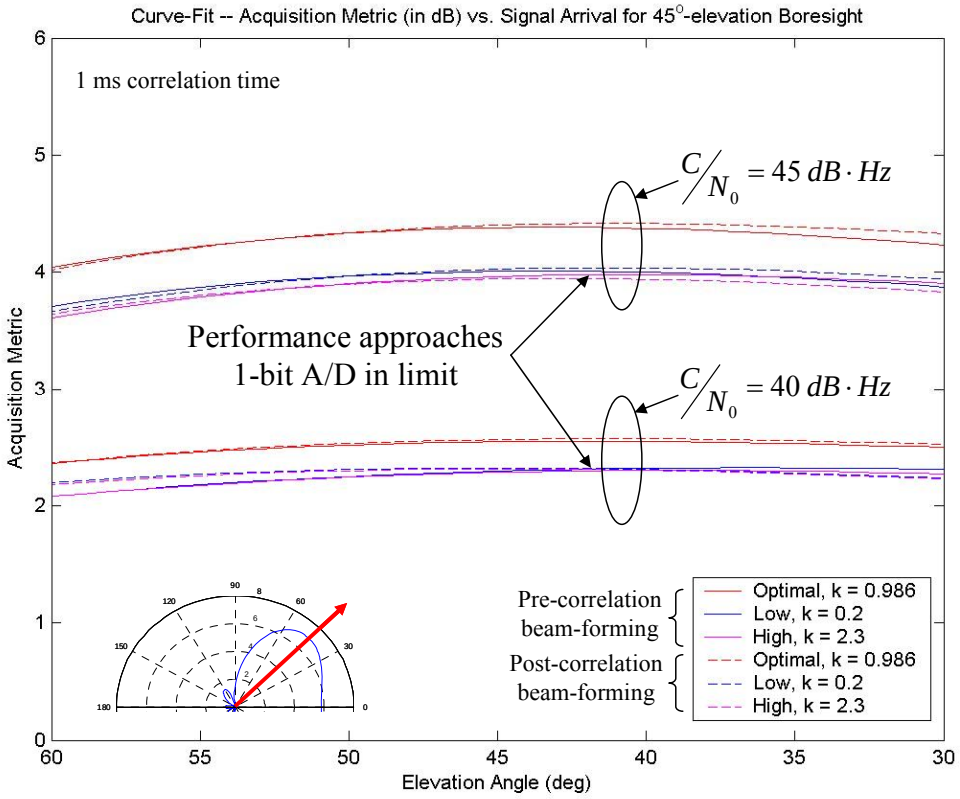

Figure 12. Correlation metric vs. ADC dynamic range and correlation architecture.

ACKNOWLEDGMENTS

The authors gratefully acknowledge the support of the JPALS Program Office, and the Naval Air Warfare Center Aircraft Division through contract N00421-01-C-0022.

REFERENCES

[Akos & Tsui, 1996], D.M. Akos and J.B.Y. Tsui, "Design and Implementation of a Direct Digitization GPS Receiver Front End," *IEEE Transactions on Microwave Theory and Techniques*, vol. 44, no. 12, pp. 2334-2339, Dec. 1996.

[Akos, 2000], D.M. Akos, P.-L. Normark, J.-T. Lee, K.G. Gromov, J.B.Y. Tsui, and J. Schamus, "Low Power Global Navigation Satellite System (GNSS) Signal Detection and Processing," *Proc. ION GPS 2000*, pp. 784-791, Sept. 2000.

[Amoroso, 1983], F. Amoroso, "Adaptive A/D Converter to Suppress CW Interference in DSPN Spread-Spectrum Communications," *IEEE Transactions on Communications*, vol. 31, no. 10, pp. 1117-1123, Oct. 1983.

[Amoroso & Bricker, 1986], F. Amoroso and J.L. Bricker, "Performance of the Adaptive A/D Converter in Combined CW and Gaussian Interference," *IEEE Transactions on Communications*, vol. 34, no. 3, pp. 209-213, March 1986.

[Applebaum, 1976], S.P. Applebaum, "Adaptive Arrays," *IEEE Transactions on Antennas and Propagation*, vol. 24, no. 5, pp. 585-598, Sept. 1976.

[Bastide, 2003], F. Bastide, D. Akos, C. Macabiau, and B. Roturier, "Automatic Gain Control (AGC) as an Interference Assessment Tool," *Proc. ION GNSS 2003*, Sept. 2003.

[Granados, 2000], G. Seco Granados, "Antenna Arrays for Multipath and Interference Mitigation in GNSS Receivers," Ph.D. Dissertation, Universitat Politècnica de Catalunya, July 2000.

[Gromov, 2002], K. Gromov, "Generalized Interference Detection and Localization System," Ph.D. Dissertation, Stanford University, March 2002.

[Jung, 2004], J. Jung, "Implementation of Correlation Power Peak Ratio Based Signal Detection Method," *Proc. ION GNSS 2004*, in press.

[Kim & Iltis, 2002], S.-J. Kim and R.A. Iltis, "GPS C/A Code Tracking with Adaptive Beamforming and Jammer Nulling," *Proc. Thirty-Sixth Asilomar Conference on Signals, Systems, and Computers*, vol. 2, pp. 975-979, Nov. 2002.

[Kim, 2004], U.-S. Kim, D.S. De Lorenzo, J. Gautier, P. Enge, and J.A. Orr, "Phase Effects Analysis of Patch Antenna CRPAs for JPALS," *Proc. ION GNSS 2004*, in press.

[Misra & Enge, 2001], P. Misra and P. Enge, "*Global Positioning System*," Ganga-Jamuna Press, 2001.

[Prades, 2004], C. Fernández Prades, A. Ramírez González, P. Closas Gómez, and J.A. Fernández Rubio, "Antenna Array Receiver for GNSS," *European Navigation Conference*, May 2004.

[Spilker, 1996], J.J. Spilker, "Fundamentals of Signal Tracking Theory," in *Global Positioning System: Theory and Applications I*, B.W. Parkinson and J.J. Spilker (Eds.), AIAA, pp. 245-327, 1996.

[Spilker & Natali, 1996], J.J. Spilker and F.D. Natali, "Interference Effects and Mitigation Techniques," in *Global Positioning System: Theory and Applications I*, B.W. Parkinson and J.J. Spilker (Eds.), AIAA, pp. 717-771, 1996.

[Stutzman & Thiele, 1998], W.L. Stutzman and G.A. Thiele, "*Antenna Theory and Design, 2nd Edition*," John Wiley & Sons, 1998.

[Van Dierendonck, 1996], A.J. Van Dierendonck, "GPS Receivers," in *Global Positioning System: Theory and Applications I*, B.W. Parkinson and J.J. Spilker (Eds.), AIAA, pp. 329-407, 1996.

[Ward, 1996a], P. Ward, "Satellite Signal Acquisition and Tracking," in *Understanding GPS: Principles and Applications*, D. Kaplan (Ed.), Artech House, pp. 119-208, 1996.

[Ward, 1996b], P. Ward, "Effects of RF Interference on GPS Satellite Signal Receiver Tracking," in *Understanding GPS: Principles and Applications*, D. Kaplan (Ed.), Artech House, pp. 209-236, 1996.